Mechanism of Cu^+-transporting ATPases: Soluble Cu^+ chaperones directly transfer Cu^+ to transmembrane transport sites

Manuel González-Guerrero and José M. Argüello*

Department of Chemistry and Biochemistry, Worcester Polytechnic Institute, 100 Institute Road, Worcester, MA 01609

Edited by Robert M. Stroud, University of California, San Francisco, CA and approved February 20, 2008 (received for review December 4, 2007)

As in other P-type ATPases, metal binding to transmembrane metal-binding sites (TM-MBS) in Cu^+-ATPases is required for enzyme phosphorylation and subsequent transport. However, Cu^+ does not access Cu^+-ATPases in a free (hydrated) form but is bound to a chaperone protein. Cu^+ transfer from Cu^+ chaperones to regulatory cytoplasmic metal-binding domains (MBDs) present in these ATPases has been described, but there is no evidence of a proposed subsequent Cu^+ movement from the MBDs to the TM-MBS. Alternatively, we postulate the parsimonious Cu^+ transfer by the chaperone directly to TM-MBS. Testing both models, the delivery of Cu^+ by *Archaeoglobus fulgidus* Cu^+ chaperone CopZ to the corresponding Cu^+-ATPase, CopA, was studied. As expected, CopZ interacted with and delivered the metal to CopA MBDs. Cu^+-loaded MBDs, acting as metal donors, were unable to activate CopA or a truncated CopA lacking MBDs. Conversely, Cu^+-loaded CopZ activated the CopA ATPase and CopA constructs in which MBDs were rendered unable to bind Cu^+. Furthermore, under nonturnover conditions, CopZ transferred Cu^+ to the TM-MBS of a CopA lacking MBDs. These data are consistent with a model where MBDs serve a regulatory function without participating in metal transport and the chaperone delivers Cu^+ directly to transmembrane transport sites of Cu^+-ATPases.

CopA | CopZ | Cu homeostasis | Cu-ATPase | metal binding

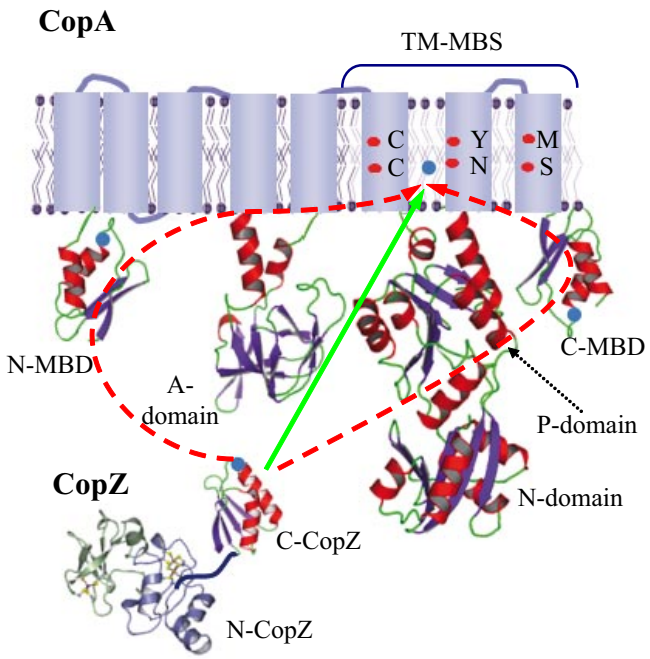

Fig. 1. Scheme of CopA and CopZ structures and hypothetical models for Cu^+ delivery to TM-MBS. The topological scheme of CopA includes the A-domain [Protein Data Bank (PDB) ID code 2HC8] and ATP-BD (PDB ID code 2B8E) structures. N-MBD and C-MBD structures are homology models based on the fourth N-MBD of the Menkes protein (PDB ID code 1AW0) and *Bacillus subtilis* CopZ (PDB ID code 1K0V), respectively. Amino acids involved in the Cu^+ coordination by the TM-MBS are indicated. CopZ scheme includes the N-CopZ structure (PDB ID code 2HU9) and the C-CopZ homology model based on *Enterococcus hirae* CopZ (PDB ID code 1CPZ). The green continuous line represents the direct delivery of Cu^+ by CopZ to TM-MBS. The red dotted lines symbolize the Cu^+ transfer from CopZ to N-MBD and C-MBD and the subsequent relocation of Cu^+ from the MBDs to the TM-MBS.

Copper is an essential cofactor in many biological processes (1). However, it also participates in harmful Fenton reactions. Consequently, Cu is "buffered" at a "no-free Cu" level by metallothioneins and chaperones with binding constants for Cu^+ in the picomolar–femtomolar range (2, 3). Within these constraints, Cu^+ chaperones route Cu^+ to various intracellular targets, and Cu^+ transmembrane transport systems maintain the total copper quota within the 10–100 μM range (1–4). How the Cu^+ chaperones transfer the metal to and from transmembrane transport sites is a central feature of transmembrane Cu^+ transport. To better understand these phenomena, we have studied the delivery of Cu^+ by the *Archaeoglobus fulgidus* Cu^+ chaperone, CopZ, to the corresponding Cu^+-ATPase, CopA.

CopA is a member of the P_{1B} subgroup of P-type ATPases (5–7). Cu^+-ATPases are essential to maintain Cu^+ homeostasis. For instance, mutations in the two Cu^+-ATPase genes present in humans, ATP7A and ATP7B, lead to Menkes syndrome and Wilson's disease, respectively (8, 9). The Cu^+-ATPases transport cycle follows the classical E1/E2 Albers–Post model (10–12). Catalytic phosphorylation of the enzyme in the E1 conformation occurs upon binding of cytoplasmic metal to transmembrane metal-binding sites (TM-MBS) and ATP binding with high affinity (l μM) to the ATP-binding domain (ATP-BD) (Fig. 1). It is assumed that upon phosphorylation, Cu^+ is occluded within the transmembrane region. The subsequent conformational change allows metal deocclusion and release to the extracellular (vesicular/luminal) compartment followed by enzyme dephosphorylation and return to the E1 form (10). Functional studies of various Cu^+-ATPases have characterized the Cu^+ transport, Cu^+-dependent ATPase activity, phosphorylation, and dephosphorylation partial reactions (5, 13–19).

Cu^+-ATPases consist of eight transmembrane segments, two large cytosolic loops comprising the A-domain and the ATP-BD, and regulatory metal-binding domains (MBDs) in their N terminus (6, 8–10, 20, 21) (Fig. 1). *A. fulgidus* CopA has an atypical

Author contributions: J.M.A. designed research; M.G.-G. performed research; M.G.-G. and J.M.A. analyzed data; and M.G.-G. and J.M.A. wrote the paper.

The authors declare no conflict of interest.

This article is a PNAS Direct Submission.

*To whom correspondence should be addressed. E-mail: arguello@wpi.edu.

This article contains supporting information online at www.pnas.org/cgi/content/full/0711446105/DCSupplemental.

additional MBD in its C terminus. MBDs are 60- to 70-aa-long domains. They have a $\beta\alpha\beta\beta\alpha\beta$ fold and an invariant CXXC metal-binding sequence similar to the well described Cu^+ chaperones, Atox1, Atx1, and CopZ (20, 22, 23). N-MBDs bind Cu^+ with high affinity (24–26), and *in vivo*, they receive Cu^+ from the corresponding Cu^+ chaperones (23, 27, 28). In bacterial Cu^+-ATPases, deletion of these domains or mutation of Cu^+-binding Cys residues does not prevent metal activation of the ATPase, although they affect enzyme turnover rate (15, 16, 19). Significantly, N-MBDs appear necessary for ATPase metal-dependent targeting and localization in eukaryote systems (9). Invariant amino acids present in transmembrane helices H6 (two Cys), H7 (Asn, Tyr), and H8 (Met, Ser) constitute the TM-MBS (Fig. 1) responsible for ion translocation (10, 16, 17). Mutation of any of these residues leads to enzyme inactivation by preventing all Cu^+-dependent catalytic steps. Metal specificity is determined by the TM-MBS rather than the MBDs. Thus, removal by MBD metal-binding capability does not affect the metal selectivity of P_{1B}-ATPases (16, 29–31).

It has been well established for classical P-type ATPases (Ca^{2+}-ATPase or Na^+,K^+-ATPase) that binding of free cytoplasmic cations at the TM-MBS is a critical reaction in the transport mechanism. However, Cu^+ does not access the ATPase as a free (hydrated) ion but is bound to a chaperone protein. Cu^+ chaperones that deliver metal specifically to Cu^+-ATPases have been identified in a range of organisms (4, 20, 22). We recently described the *A. fulgidus* Cu^+ chaperone CopZ (32). CopZ contains a C-terminal Cu^+ chaperone domain (C-CopZ) homologous to the eukaryote and bacterial chaperones (Fig. 1). In addition, CopZ has an unusual 130-aa Cys-rich N-terminal domain (N-CopZ) containing a [2Fe–2S] cluster and a Zn^{2+}-binding site. The transfer of Cu^+ from Cu^+ chaperones to Cu^+-ATPase N-MBDs has been extensively characterized (9, 14, 18, 27, 28, 32, 33). Most of these studies have built on a model where a thermodynamically shallow gradient allows for Cu^+ routing from the chaperone to MBDs and from these to the TM-MBS (represented by dashed red lines in Fig. 1). The net Cu^+ flux among these sites would be kinetically driven by metal translocation across the membrane, a process energized by ATP (28). Supporting this model, the second MBD of the Wilson protein appears to be required for Cu^+-dependent phosphorylation by ATP by using Atox1·Cu^+ as metal donor (18). In addition, MBDs seem essential for Wilson's disease protein function when it is examined in yeast functional complementation studies (34). However, transfer of Cu^+ from an MBD to the TM-MBS has not been shown. Moreover, considering that in bacterial ATPases, removal of N-MBDs or mutation of their metal-binding Cys residues does not result in loss of transport (15, 16, 19), an alternative parsimonious model appears plausible. In this model, the chaperone would "directly" deliver the metal to the TM-MBS by docking with the exposed metal entrance to the TM-MBS (represented by a green line in Fig. 1). This direct delivery process would be independent of a nonessential regulatory chaperone/MBD Cu^+ exchange.

Here, we present evidence that differentiates between these models and shows the role of the Cu^+ chaperone in delivery of metal to transmembrane transport sites of Cu^+-ATPases. Furthermore, the data reveal distinct mechanistic features that differentiate P_{1B}-ATPases from classical alkali metal-transporting P-ATPases.

Results

Cu^+ Binding to CopA MBDs and CopZ. We initiated these studies by characterizing the interaction of Cu^+ with *A. fulgidus* CopA MBDs and CopZ. CopA has two cytosolic MBDs, N-MBD and C-MBD (Fig. 1). These MBDs were expressed and purified separately as soluble polypeptides, and Cu^+ binding was studied in the presence of the Cu^+ indicator bicinchoninic acid (BCA).

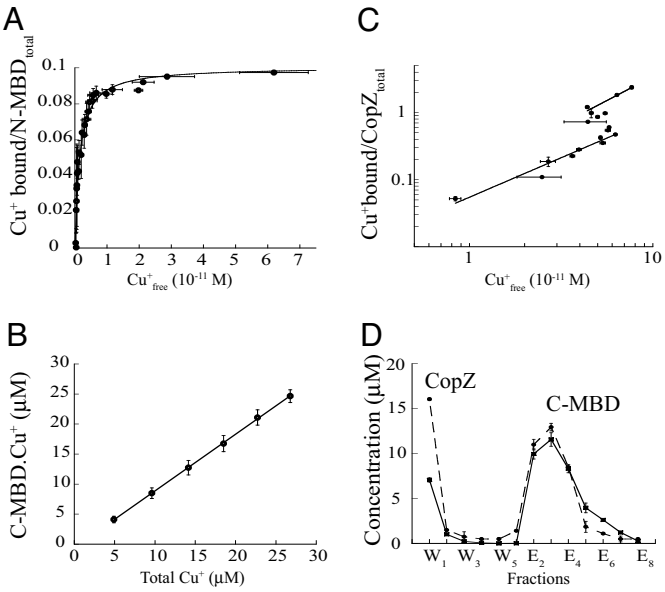

Fig. 2. Cu^+ binding to and Cu^+ transfer between cytosolic MBDs and CopZ. (*A–C*) Cu^+ binding to N-MBD (*A*), C-MBD (*B*), and CopZ (*C*), determined in protein/BCA competition assays. The data were fit by using $n = 0.12 \pm 0.02$ and $K_a = 6.8 \pm 0.8 \times 10^{11}$ M^{-1} for N-MBD·Cu^+, and $n_1 = 1.2 \pm 0.2$, $K_{a1} = 4.8 \pm 1.1$ 10^{11} M^{-1}, $n_2 = 1.3 \pm 0.1$, $K_{a2} = 6.6 \pm 2.2$ 10^{14} M^{-1} for CopZ·Cu^+. C-MBD data were fit to [C-MBD·Cu^+] = n[Cu^+], with $n = 0.94 \pm 0.04$. Values are the mean ± SE ($n = 3$). (*D*) Copper transfer from CopZ to isolated C-MBD. The copper (●) and protein (■) content of the wash (W) and elution (E) fractions are shown. Peaks corresponding to specific proteins eluted from the streptactin column are identified.

Both domains were able to bind Cu^+, although with significantly different affinities (Fig. 2 *A* and *B*). N-MBD bound Cu^+ with a K_a of $6.8 \pm 0.8 \times 10^{11}$ M^{-1}, whereas C-MBD completely displaced Cu^+ from the competing BCA. Although an accurate determination of C-MBD·Cu^+ K_a was not possible, it appears to be significantly higher than that of the BCA_2·Cu^+ ($K_a = 4.6 \times 10^{14}$ M^{-2}). Sazinsky *et al.* (32) showed that CopZ has a Cu^+-binding site in the chaperoning C-CopZ domain, but the Fe-S-containing N-CopZ domain binds an additional Cu^+ during *in vitro* Cu^+ loading of CopZ. Consequently, Fig. 2*C* shows the binding of Cu^+ to CopZ with two different K_a values: 6.6 ± 2.2 10^{14} M^{-1} and 4.8 ± 1.1 10^{11} M^{-1} for the C-CopZ and N-CopZ, respectively. Comparable values have been estimated for other Cu^+ chaperones and N-MBDs (3, 26, 35). However, lower K_a values have been obtained in studies of similar domains by using alternative methodologies (24, 36). Consequently, the emphasis here will be placed on the comparative analysis of Cu^+-binding parameters of CopZ and CopA domains obtained with the same method.

Chaperone-mediated delivery of Cu^+ to cytosolic MBDs has been shown for a number of chaperone/ATPase pairs (14, 28, 32). In the case of *A. fulgidus* CopZ and CopA, we have shown that CopZ delivers Cu^+ to the isolated N-MBD of CopA, albeit with a small apparent K_{eq} (32). Considering the possible role of the C-MBD in Cu^+ delivery to the TM-MBS, we assessed the transfer of Cu^+ from CopZ to this domain (Fig. 2*D*). In agreement with the relative K_a, CopZ was able to donate Cu^+ to the C-MBD more efficiently than to the N-MBD. This cation transfer appears to occur through specific protein interaction rather than via Cu^+ dissociation from CopZ and subsequent binding to the MBDs. Supporting this contention, when control experiments were performed in the absence of Cu^+ acceptors, <10% of Cu^+ dissociated from CopZ·Cu^+ after 10 min at room temperature. Similarly, CopZ·Cu^+ dissociation was minimal

BIOCHEMISTRY

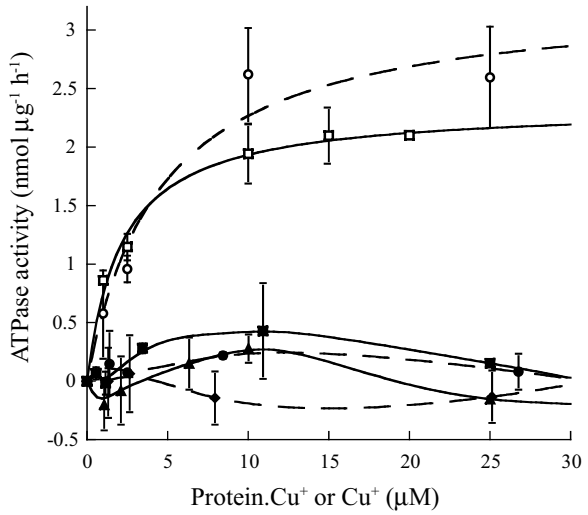

Fig. 3. ΔN,C-CopA (□, ■, ▲) and CopA (○, ●, ♦) ATPase activity in the presence of N-MBD·Cu^+ or C-MBD·Cu^+. Cu^+ was included in the assay medium as a free species (□, ○), bound to N-MBD (■, ●) or to C-MBD (▲, ♦). Data of Cu^+ activation of ΔN,C-CopA were fitted by using $K_{1/2}$ = 2.2 ± 0.3 μM and V_{max} = 2.4 ± 0.1 nmol μg^{-1} h^{-1}. Data of Cu^+ activation of CopA were fitted by using $K_{1/2}$ = 4.5 ± 1.8 μM and V_{max} = 3.2 ± 0.4 nmol μg^{-1} h^{-1}. No fitting was attempted for N-MBD and C-MBD data. Values are the mean ± SE (n = 3).

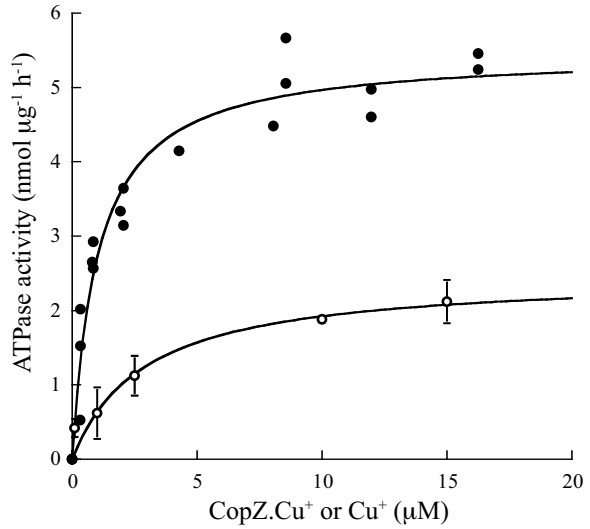

Fig. 4. CopZ·Cu^+ activation of CopA ATPase activity. Cu^+ was included in the assay medium as a free species (○) or bound to CopZ (●). Data were fitted by using the following parameters: free Cu^+, $K_{1/2}$ = 2.9 ± 1.0 μM and V_{max} = 2.5 ± 0.3 nmol μg^{-1} h^{-1}; CopZ·Cu, $K_{1/2}$ = 1.0 ± 0.2 μM and V_{max} = 5.5 ± 0.2 nmol μg^{-1} h^{-1}. Values obtained for CopZ·Cu^+ were obtained in duplicate in three independent experiments. Data obtained for free Cu^+ are the mean ± SE (n = 3).

(<10%) if the protein was dialyzed against a C-MBD containing buffer [see supporting information (SI) *Materials and Methods* and Fig. S1].

Cu^+-Bound N-MBD or C-MBD Does Not Activate CopA Cu^+-Dependent Turnover. The "indirect" model depicted in Fig. 1 implies that a cytosolic MBD, upon receiving Cu^+ from CopZ, is able to donate the metal to the TM-MBS. To test this hypothesis, the activation of CopA lacking both N-MBD and C-MBD (ΔN,C-CopA) by isolated soluble Cu^+-loaded MBDs was determined. ΔN,C-CopA retained a Cu^+-ATPase activity similar to that of wild-type CopA when measured in the presence of Cu^+ (Fig. 3 and Fig. S2*A*). However, no ATPase activation by either N-MBD·Cu^+ or C-MBD·Cu^+ was observed, even with a 100× molar excess of MBD·Cu^+ over CopA. Furthermore, control experiments showed that little or no MBD·Cu^+ dissociation occurred under the assay conditions (see Fig. S3). These ATPase activity experiments strongly suggest that MBDs cannot effectively deliver Cu^+ to TM-MBS. Nevertheless, it might be argued that: (*i*) a particular interaction between MBDs and the transmembrane region is necessary for Cu^+ transfer to TM-MBS and subsequent activation; and (*ii*) this interaction might not be achieved by the isolated soluble domains and ΔN,C-CopA. This argument is unlikely to be valid because isolated MBD·Cu^+ was also unable to activate wild-type CopA (Fig. 3 and Fig. S2*B*), although a large molar excess of MBD·Cu^+ (up to 100:1) guaranteed saturation of CopA MBD sites without a significant decrease in the availability of soluble MBD·Cu^+.

Cu^+-Bound CopZ Activates CopA Cu^+-Dependent Turnover Independently of N-MBD and C-MBD. Lutsenko and co-workers (14, 18) have shown the role of Cu^+ chaperones in activating Cu^+-ATPases by establishing that Cu^+-loaded Atox1 drives Wilson protein phosphorylation by ATP. Taking advantage of the full functionality of CopA, we measured ATPase activation by CopZ·Cu^+ acting as single Cu^+ donor. As expected, the Cu^+ chaperone drove CopA turnover (Fig. 4). Interestingly, the enzyme V_{max} in the presence of CopZ·Cu^+ was significantly higher than that observed in the presence of Cu^+. However, the $K_{1/2}$ for activation was similar for both Cu^+ and CopZ·Cu^+. Because only a small amount of Cu^+ dissociated from CopZ during the assay (<15%; see Fig. S1), the data in Fig. 4 indicate that CopZ·Cu^+ specifically interacts with and activates CopA. However, considering the large activation by CopZ·Cu^+, it could be argued that Cu^+-free CopZ is acting as a Cu^+ acceptor at an externally facing metal site. In this role, CopZ might accelerate Cu^+ release, likely a rate-limiting step (5). To test this possibility, we examined the effect of Cu^+-free CopZ on CopA activation (Fig. 5). In these experiments, ATPase activity was tested in the presence of fixed CopZ·Cu^+ concentrations yielding 50 or 100% maximal activity, whereas increasing amounts of Cu^+-free CopZ were included in the reaction medium. Under both conditions, CopA ATPase activity was not affected by the addition of

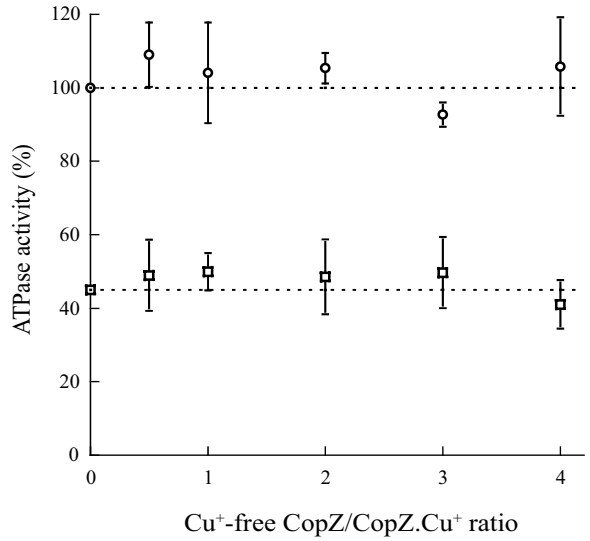

Fig. 5. Effect of Cu^+-free CopZ on CopZ·Cu^+-dependent ATPase activity of CopA. CopA ATPase activity was measured in the presence of 5 μM CopZ·Cu^+ (○) or 1.25 μM CopZ·Cu^+ (□) and Cu^+-free CopZ at the indicated molar ratios. One hundred percent activity = 4.7 ± 0.2 nmol μg^{-1} h^{-1}. Dotted lines indicate activity in the absence of Cu^+-free CopZ. Values are the mean ± SE (n = 3).

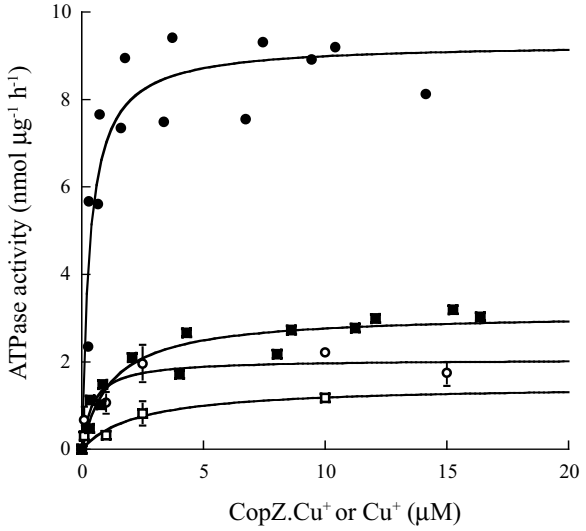

Fig. 6. CopZ·Cu^+ activation of ΔN,C-CopA and $C^{27,30,751,754}$A CopA ATPase activity. Cu^+ was included in the assay medium either as a free species (○, □) or bound to CopZ (●, ■). Data correspond to either ΔN,C-CopA (○, ●) or $C^{27,30,751,754}$A CopA (□, ■). Data were fitted by using the following parameters: ΔN,C-CopA plus free Cu^+, $K_{1/2} = 2.4 \pm 1.2$ μM and $V_{max} = 2.2 \pm 0.4$ nmol μg^{-1} h^{-1}; ΔN,C-CopA plus CopZ·Cu, $K_{1/2} = 0.3 \pm 0.1$ μM and $V_{max} = 9.3 \pm 0.4$ nmol μg^{-1} h^{-1}; for $C^{27,30,751,754}$A CopA plus free Cu^+, $K_{1/2} = 2.3 \pm 1.4$ μM and $V_{max} = 1.2 \pm 0.3$ nmol μg^{-1} h^{-1}; for $C^{27,30,751,754}$A plus CopA CopZ·Cu, $K_{1/2} = 1.0 \pm 0.3$ μM and $V_{max} = 3.1 \pm 0.2$ nmol μg^{-1} h^{-1}. Values obtained for CopZ·Cu^+ were obtained in duplicate in three independent experiments. Data obtained for free Cu^+ are the mean ± SE ($n = 3$).

Cu^+-free CopZ. These results support the idea that Cu^+-free CopZ does not affect Cu^+ release. Moreover, Cu^+-free CopZ did not decrease the activity, suggesting that it does not compete with CopZ·Cu^+ for a putative docking site close to the TM-MBS.

The observed activation of CopA by CopZ·Cu^+ indicates a direct interaction and Cu^+ transfer between these proteins. If Cu^+ directly transfers from CopZ·Cu^+ to transport sites (Fig. 1), CopZ·Cu^+ should activate CopA lacking functional MBDs (ΔN,C-CopA) and CopA in which critical Cys residues in MBDs have been mutated to Ala ($C^{27,30,751,754}$A CopA). Fig. 6 shows that both proteins hydrolyze ATP in the presence of CopZ·Cu^+. As in the case of full-length wild-type CopA, activation by CopZ·Cu^+ resulted in a significantly higher V_{max} than observed in the presence of free Cu^+. Thus, the data strongly support the transfer of Cu^+ from CopZ to CopA TM-MBS independently of MBDs.

CopZ Delivers Cu^+ to the TM-MBS of CopA. Our CopA preparations consist of the proteins solubilized in mixed lipid/detergent micelles. These CopA forms are suitable to perform Cu^+ transfer experiments in a manner similar to that used to measure soluble CopZ-MBD Cu^+ exchange. Toward this end, Cu^+ transfer was measured by incubation of CopZ·Cu^+ with apo-ΔN,C-CopA under nonturnover conditions: i.e., no Mg^{2+}-ATP. Fig. 7 shows that elution of Cu^+-bound ΔN,C-CopA was observed in these experiments. Because the TM-MBS is the only Cu^+ site in ΔN,C-CopA, the direct delivery model for Cu^+ transfer can be assumed. In agreement with the data in Fig. 5, this result also indicates that: (*i*) TM-MBS·Cu^+ K_a is much higher than that of CopZ·Cu^+; and (*ii*) Cu^+ transfer is essentially irreversible because Cu^+ is still bound to ΔN,C-CopA after relatively slow washing and column elution. Preliminary experiments indicate a K_a in the femtomolar range for the TM-MBS·Cu^+ (E. Eren, M.G.-G., and J.M.A., unpublished results). However, because assay conditions (4°C, 2.6:1 CopZ·Cu^+:CopA molar ratio) cannot assure saturation of TM-MBS, conclusions on binding stoichiometry cannot be drawn. Nonetheless, the apparent high Cu^+-binding affinity would seem to support the two conclusions above.

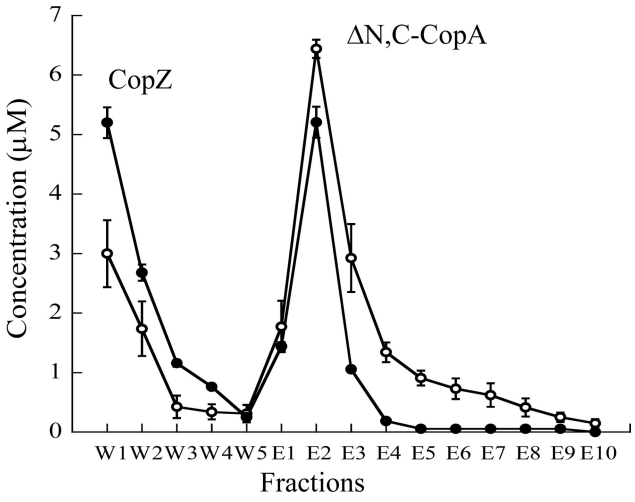

Fig. 7. Copper transfer from CopZ to ΔN,C-CopA. The copper (●) and protein (○) content of the wash (W) and elution (E) fractions are shown. Peaks corresponding to specific proteins eluted from the Ni^{2+}-nitrilotriacetic acid column are identified.

Discussion

CopZ Transfers Cu^+ Directly to the TM-MBS. The central element of transmembrane metal transport by Cu^+-ATPases is metal binding to the TM-MBS. This site determines metal specificity and is where metal translocation occurs. The goal of this work was to test alternative models for Cu^+ delivery to the TM-MBS (Fig. 1), a process that does not rely on free metal diffusion as in alkali metal-transporting ATPases but on the specific interaction between two proteins, a Cu^+ chaperone and its corresponding Cu^+-ATPase. For these studies, the *A. fulgidus* CopZ/CopA system was used.

Initial experiments characterized Cu^+ transfer from CopZ to both MBDs present in CopA. In agreement with their relative protein·Cu^+ association constants, the transfer reaction CopZ·Cu^+ + N-MBD ↔ CopZ + N-MBD·Cu^+ exists in a sizeable equilibrium (32). Consequently, occupancy of N-MBD Cu^+ sites would depend on the level of CopZ·Cu^+. A similar situation probably applies to other ATPases where $K_{eq} \approx 0.5–1.5$ has been observed for Cu^+ exchange (14, 26, 28). Along these lines, mutation of N-MBD Cys leads to a significant reduction in ATPase turnover rate (16), and truncation of these domains yields a higher enzymatic activity (37), particularly during CopZ·Cu^+ activation (Fig. 6). These observations provide further support for a regulatory mechanism in which a rise in Cu^+ levels would lead to an increase of the chaperone·Cu^+ pool, subsequent Cu^+ transfer to N-MBDs, displacement of N-MBD·Cu^+ from a slow turnover conformation (perhaps providing better access of the chaperone to the TM-MBS), and a resulting higher Cu^+-ATPase turnover/transport rate (14, 16, 18, 19). However, in the particular case of *A. fulgidus* CopA, little CopZ·Cu^+ excess saturates the C-MBD-binding sites, indicating a $K_{eq} \gg 1$ for CopZ·Cu^+ + C-MBD ↔ CopZ + C-MBD·Cu^+. Then, *in vivo* saturation of C-MBD Cu^+ sites would occur before significant CopZ·Cu^+ levels would be present, so C-MBDs would not "sense" the CopZ·Cu^+ concentration. Interestingly, mutation of the two Cys in C-MBD, i.e., removal of its Cu^+-binding capacity, had no detectable effect on enzyme activity (16).

To identify the species donating Cu^+ to the CopA TM-MBS,

BIOCHEMISTRY

activation of wild-type CopA ATPase by Cu^+-loaded CopZ, N-MBD, and C-MBD was tested. An excess of added Cu^+-bound cytoplasmic domains (N-MBD or C-MBD) was unable to activate either CopA or ΔN,C-CopA. This observation strongly supports the idea that Cu^+ bound to MBDs cannot subsequently be transferred to the TM-MBS. Alternatively, because CopZ·Cu^+ activated both enzymes, it appears that CopZ delivers Cu^+ to the TM-MBS independently of the presence of functional MBDs in the ATPase. Further supporting this model, CopZ·Cu^+ transferred the metal to ΔN,C-CopA, an enzyme where only the TM-MBS remains as a Cu^+ acceptor.

Considering alternative mechanisms, previous studies have shown that chaperone·Cu^+-dependent Wilson's disease protein phosphorylation requires at least a functional MBD2 (18). As suggested by the authors, in this case, Cu^+ binding might be required to displace MBD2 from blocking access of the chaperone·Cu^+ to the TM-MBS (18). On the other hand, multi-MBD eukaryotic proteins and single-MBD prokaryotic/archaeal proteins might have different transport mechanisms. For instance, it could be postulated that, upon Cu^+ binding, the multi-MBD N terminus undergoes a conformational change that directs a N-MBD·Cu^+ to the membrane. However, our data suggest that this and other alternative mechanisms are not the most appropriate model, but they do support a mechanism where CopZ (rather than MBDs) delivers Cu^+ to TM-MBS.

CopZ–CopA Interaction. Although the chaperone domain of CopZ and CopA MBDs are highly homologous and share a similar structure, only CopZ is able to deliver Cu^+ to the TM-MBS. Moreover, CopA does not appear to interact with Cu^+-free CopZ. Instead, CopA seems to discriminate between quite similar structures: Cu^+-free CopZ and CopZ·Cu^+. In this regard, Ca^{+2}-ATPases present a "funnel"-like structure, comprised of H1, H3, and the A-domain (12, 38), in the cytoplasmic access to Glu^{309}, the first residue in the Ca^{2+}-ATPase TM-MBS. A similar architecture might be present in Cu^+-ATPases, where the ends of H3 (equivalent to H1 of SERCA1), H5 (equivalent to H3 of SERCA1), and the A-domain might constitute a docking site for CopZ·Cu^+ and direct Cu^+ transfer to Cys^{382} (the functional analogue of Glu^{309} in SERCA1).

Mechanism of Cu^+ Transport. Our experiments also illustrate mechanistic aspects of the Cu^+-ATPases. In the case of the Ca^{2+}- and Na^+,K^+-ATPases, transported cations bind reversibly, and protein phosphorylation is required to prevent cytoplasmic release of the outwardly transported ions (11, 12). The CopZ/ΔN,C-CopA Cu^+ transfer experiment indicates that in Cu^+-ATPases, metal binding to the cytoplasm facing TM-MBS is essentially irreversible. This property is likely achieved by the tight Cu^+ binding (via a quite small k_{off}) and the apparent low-affinity interaction of Cu^+-free CopZ with its docking site in CopA. In this case, protein phosphorylation is not required to prevent the backward ion release; however, the Cu^+-bound CopA form obtained in the absence of other ligands might not necessarily be equivalent to the cation-occluded transitional conformations described for P_2-ATPases (11, 12). Studies exploring Cu^+ coordination during transport might clarify this point.

On the other hand, the vectorial transfer of Cu^+ from CopZ to CopA TM-MBS and the largely irreversible Cu^+ binding to TM-MBS imply a high TM-MBS·Cu^+ K_a value. This might be seen to be in discordance with Cu^+ and CopZ·Cu^+ $K_{1/2}$ for ATPase activation in the micromolar range. However, the TM-MBS·Cu^+ K_a reflects only the Cu^+ + TM-MBS ↔ TM-MBS·Cu^+ equilibrium, whereas $K_{1/2}$ for activation is the product of multiple equilibriums in the catalytic cycle. For instance, CopA in the E1 form, available for Cu^+ binding, depends on the E1↔ E2 equilibrium; alternatively, the TM-MBS·Cu^+ CopA form will be phosphorylated and depend on the E1P(Cu^+) ↔ E2P + Cu^+ equilibrium.

Summary. The experiments described here show that the Cu^+ chaperone CopZ delivers Cu^+ to the Cu^+-ATPase transmembrane transport sites. Regulatory cytoplasmic MBDs cannot perform this function. Cu^+-ATPase mechanistic characteristics (essentially irreversible metal binding to TM-MBS and high turnover in the presence of Cu^+ chaperone) lead to efficient outward vectorial transport with minimum inward leakage of free metal.

Materials and Methods

cDNA Cloning, Protein Expression, and Purification. *A. fulgidus* CopA, CopZ, and $C^{27,30,751,754}$A CopA cDNAs were obtained as described (5, 16, 32). A construct encoding for truncated CopA extending from Gly^{80} to Gly^{736} and therefore lacking the N-MBD and C-MBD (ΔN,C-CopA) was obtained by PCR by using CopA as template. The resulting cDNA was cloned in pBAD-TOPO vector (Invitrogen), which adds a C terminus His tag sequence. cDNAs coding for the first 77 aa of CopA, Met^1–Leu^{77} (N-MBD), and the last 80 aa, Leu^{725}–Ser^{804} (C-MBD), were obtained by PCR by using CopA cDNA as template. These cDNAs were digested with BsaI and cloned in pPRIBA1 (IBA), which adds a C terminus streptavidin (Strep) tag sequence. Protein expression was induced for 3 h by the addition of 0.02% arabinose to cells containing pBAD-TOPO-based vectors or 1 mM isopropyl-β-D-thiogalactopyranoside to cells harboring pCRT7/NT-TOPO and pPRIBA1-based plasmids.

Membrane-bound proteins, CopA, $C^{27,30,751,754}$A CopA, and ΔN,C-CopA, were prepared as described in ref. 5. In all experiments, these proteins were in soluble form stabilized in mixed 0.01% dodecyl-β-D-maltoside (DDM), 0.01% asolectin micelles. Cells expressing soluble proteins, N-MBD, C-MBD, and CopZ, were disrupted by sonication in 100 mM Tris (pH 8.0), 150 mM NaCl, and homogenates were centrifuged at 10,000 × *g* for 30 min. The resulting supernatants were centrifuged at 110,000 × *g* for 60 min. CopZ-His was purified by using a Ni^{2+}-nitrilotriacetic acid column and stored in 25 mM Tris (pH 8.0), 100 mM sucrose, 50 mM NaCl, and 10 mM ascorbate. N-MBD, C-MBD, and CopZ-Strep were purified by passage through a Strep-Tactin SuperFlow column (IBA). These proteins were stored in 100 mM Tris (pH 8.0), 150 mM NaCl, and 10 mM ascorbate at −80°C. Protein determinations were performed in accordance with Bradford (39).

Cu^+ Loading to Proteins. Cu^+ loading to apo N-MBD, C-MBD, and CopZ was performed by incubating each protein in the presence of a 10-fold molar excess of $CuSO_4$, 25 mM Hepes (pH 8.0), 150 mM NaCl, and 10 mM ascorbate for 10 min at room temperature with gentle agitation. The unbound Cu^+ was removed by passing through a Sephadex G-10 column (Sigma). The amount of Cu^+ bound was determined by the BCA method (40). $CuSO_4$ solutions were used as standards.

Cu^+-Binding Affinity. Protein·Cu^+ K_a values were determined by using a competition assay with BCA followed by colorimetric determination of the BCA_2·Cu^+ complex at 360 nm. Because of the different Cu^+ affinities of the studied proteins, various approaches were used. N-MBD·Cu^+ K_a was determined by titrating with BCA in a solution of 10 μM Cu^+, 100 μM N-MBD in 50 mM Hepes (pH 7.5), 200 mM NaCl, and 200 μM ascorbate (buffer H). C-MBD·Cu^+ K_a was determined by titrating with Cu^+ in a solution of 25 μM C-MBD, 250 μM BCA in buffer H. CopZ K_a values were obtained by titrating with Cu^+ in a solution of 20 μM BCA, 80 μM CopZ in buffer H. The BCA_2·Cu^+ molar extinction coefficient, ε_{360} = 20,600 cm^{-1} M^{-1}, was determined by titrating 10 μM Cu^+ with 0–10 μM BCA in buffer H. Free metal concentrations were calculated from $K_{BCA} = [BCA_2{\cdot}Cu^+]/[BCA_{free}]^2[Cu^+_{free}]$, where K_{BCA} is the association constant for BCA_2·Cu^+ (4.60×10^{14} M^{-2}) (26). The N-MBD·Cu^+ and CopZ·Cu^+ K_a values were calculated by using $\nu = [Cu^+_{free}]^n K_a/(1 + K_a[Cu^+_{free}]^n)$, where ν is the molar ratio of metal bound to protein and n is the number of metal-binding sites. Reported errors for K_a and n are asymptotic standard errors provided by the fitting software (Origin; OriginLab).

Cu^+ Transfer Assay. To assess Cu^+ transfer from CopZ to C-MBD, the C-MBD was bound to Strep-Tactin resin equilibrated in 25 mM Hepes (pH 8.0), 150 mM NaCl, 10 mM ascorbic acid (buffer M). CopZ-His fully loaded with Cu^+ was added in 3-fold excess to resin-bound C-MBD CopA and incubated for 10 min at room temperature for Cu^+ exchange. Proteins were separated by washing resin columns with buffer M followed by elution with 2.5 mM desthiobiotin in buffer M. Wash and elution fractions were collected and analyzed for Cu^+ and

protein content. Cu^+ transfer from CopZ to ΔN,C-CopA was performed in a similar fashion with the exception that ΔN,C-CopA was bound to a Ni^{2+}-nitrilotriacetic acid column, and 3 M excess of Strep-tagged CopZ was used as Cu^+ donor. Proteins were separated by washing with 25 mM Hepes (pH 8.0), 100 mM sucrose, 500 mM NaCl, 0.01% DDM, 0.01% asolectin, 10 mM ascorbic acid, 20 mM imidazole followed by elution with 25 mM Hepes (pH 8.0), 100 mM sucrose, 500 mM NaCl, 0.01% DDM, 0.01% asolectin, 10 mM ascorbic acid, 300 mM imidazole. The absence of C-MBD or ΔN,C-CopA in the wash fractions and CopZ in the elution fractions was confirmed by SDS/PAGE. Controls were performed where Cu^+-loaded CopZ-His, CopZ-Strep, apoC-MBD, and ΔN,C-CopA were subjected to the same procedures individually, i.e., lacking a partner Cu^+-exchanging protein.

ATPase Assays. These were performed at 75°C in a medium containing 50 mM Tris (pH 6.1 at 75°C), 3 mM $MgCl_2$, 3 mM ATP, 0.01% asolectin, 0.01% DDM, 400 mM NaCl, 2.5 mM DTT, and 20–40 μg/ml purified protein. Cu^+ concentrations, either in the free form or bound to proteins, were varied as indicated in the corresponding figures. N-MBD·Cu^+, C-MBD·Cu^+, or CopZ·Cu^+ was used immediately after removing unbound Cu^+. Controls with apoN-MBD, C-MBD, or Cu^+-free CopZ were used as blanks when necessary. ATPase activity was measured after a a 10-min incubation, except that when N-MBD acted as Cu^+ donor, 5-min incubations were performed. Released P_i was determined according to Lanzetta *et al.* (41). ATPase activity measured in the absence of metal was subtracted from plotted values. Curves of ATPase activity vs. donor·Cu^+ (N-MBD, C-MBD, or CopZ) concentrations were fit to $v = V_{max}[\text{donor}\cdot Cu^+]/([\text{donor}\cdot Cu^+]+K_{1/2})$. The reported standard errors for V_{max} and $K_{1/2}$ are asymptotic standard errors reported by the fitting software KaleidaGraph (Synergy).

ACKNOWLEDGMENTS. We thank Drs. Elif Eren and Joshua Berlin (University of Medicine and Dentistry of New Jersey–New Jersey Medical School) for useful discussions and suggestions, Brad Kaufman for invaluable technical assistance, and Dr. Matt Sazinsky (Northwestern University) for the ΔN,C-CopA pBAD construct. This work was supported by National Science Foundation Grant MCB-0235165 (to J.M.A.).

1. Fraústro da Silva JJR, Williams RJP (2001) *The Biological Chemistry of the Elements* (Oxford Univ Press, New York), pp 418–435.
2. Changela A, *et al.* (2003) Molecular basis of metal-ion selectivity and zeptomolar sensitivity by CueR. *Science* 301:1383–1387.
3. Rae TD, Schmidt PJ, Pufahl RA, Culotta VC, O'Halloran TV (1999) Undetectable intracellular free copper: The requirement of a copper chaperone for superoxide dismutase. *Science* 284:805–808.
4. O'Halloran TV, Culotta VC (2000) Metallochaperones, an intracellular shuttle service for metal ions. *J Biol Chem* 275:25057–25060.
5. Mandal AK, Cheung WD, Argüello JM (2002) Characterization of a thermophilic P-type Ag^+/Cu^+-ATPase from the extremophile *Archaeoglobus fulgidus*. *J Biol Chem* 277:7201–7208.
6. Argüello JM (2003) Identification of ion-selectivity determinants in heavy-metal transport P_{1B}-type ATPases. *J Membr Biol* 195:93–108.
7. Axelsen KB, Palmgren MG (1998) Evolution of substrate specificities in the P-type ATPase superfamily. *J Mol Evol* 46:84–101.
8. Cox DW, Moore SDP (2002) Copper transporting P-type ATPases and human disease. *J Bioenerg Biomembr* 34:333–338.
9. Lutsenko S, Barnes NL, Bartee MY, Dmitriev OY (2007) Function and regulation of human copper-transporting ATPases. *Phys Rev* 87:1011–1046.
10. Argüello JM, Eren E, González-Guerrero M (2007) The structure and function of heavy metal transport P(1B)-ATPases. *BioMetals* 20:233–248.
11. Kaplan JH (2002) Biochemistry of Na^+,K^+-ATPase. *Annu Rev Biochem* 71:511–535.
12. Toyoshima C, Inesi G (2004) Structural basis of ion pumping by Ca(2+)-ATPase of the sarcoplasmic reticulum. *Annu Rev Biochem* 73:269–292.
13. Tsivkovskii R, Eisses JF, Kaplan JH, Lutsenko S (2002) Functional properties of the copper-transporting ATPase ATP7B (the Wilson's disease protein) expressed in insect cells. *J Biol Chem* 277:976–983.
14. Walker JM, Tsivkovskii R, Lutsenko S (2002) Metallochaperone Atox1 transfers copper to the NH_2-terminal domain of the Wilson's disease protein and regulates its catalytic activity. *J Biol Chem* 277:27953–27959.
15. Fan B, Rosen BP (2002) Biochemical characterization of CopA, the *Escherichia coli* Cu(I)-translocating P-type ATPase. *J Biol Chem* 277:46987–46992.
16. Mandal AK, Argüello JM (2003) Functional roles of metal-binding domains of the *Archaeoglobus fulgidus* Cu(+)-ATPase CopA. *Biochemistry* 42:11040–11047.
17. Mandal AK, Yang Y, Kertesz TM, Argüello JM (2004) Identification of the transmembrane metal binding site in Cu^+-transporting PIB-type ATPases. *J Biol Chem* 279:54802–54807.
18. Walker JM, *et al.* (2004) The N-terminal metal-binding site 2 of the Wilson's disease protein plays a key role in the transfer of copper from Atox1. *J Biol Chem* 279:15376–15384.
19. Voskoboinik I, *et al.* (1999) Functional analysis of the N-terminal CXXC metal-binding motifs in the human Menkes copper-transporting P-type ATPase expressed in cultured mammalian cells. *J Biol Chem* 274:22008–22012.
20. Arnesano F, *et al.* (2002) Metallochaperones and metal-transporting ATPases: A comparative analysis of sequences and structures. *Genome Res* 12:255–271.
21. Sazinsky MH, Mandal AK, Argüello JM, Rosenzweig AC (2006) Structure of the ATP-binding domain from the *Archaeoglobus fulgidus* Cu^+-ATPase. *J Biol Chem* 281:11161–11166.
22. Banci L, Bertini I, Del Conte R, Markey J, Ruiz-Dueñas FJ (2001) Copper trafficking: The solution structure of *Bacillus subtilis* CopZ. *Biochemistry* 40:15660–15668.
23. Wernimont AK, Huffman DL, Lamb AL, O'Halloran TV, Rosenzweig AC (2000) Structural basis for copper transfer by the metallochaperone for the Menkes/Wilson disease proteins. *Nat Struct Biol* 7:766–771.
24. Jensen PY, Bonander N, Möller LB, Farver O (1999) Cooperative binding of copper(I) to the metal binding domains in Menkes disease protein. *Biochim Biophys Acta* 1434:103–113.
25. Lutsenko S, Petrukhin K, Cooper MJ, Gilliam CT, Kaplan JH (1997) N-terminal domains of human copper-transporting adenosine triphosphatases (the Wilson's and Menkes disease proteins) bind copper selectively *in vivo* and *in vitro* with stoichiometry of one copper per metal-binding repeat. *J Biol Chem* 272:18939–18944.
26. Yatsunyk LA, Rosenzweig AC (2007) Cu(I) binding and transfer by the N terminus of the Wilson disease protein. *J Biol Chem* 282:8622–8631.
27. Hamza I, Schaefer M, Klomp LWJ, Gitlin JD (1999) Interaction of the copper chaperone HAH1 with the Wilson disease protein is essential for copper homeostasis. *Proc Natl Acad Sci USA* 96:13363–13368.
28. Huffman DL, O'Halloran TV (2000) Energetics of copper trafficking between the Atx1 metallochaperone and the intracellular copper transporter, Ccc2. *J Biol Chem* 275:18611–18614.
29. Mana-Capelli S, Mandal AK, Argüello JM (2003) *Archaeoglobus fulgidus* CopB is a thermophilic Cu^{2+}-ATPase: Functional role of its histidine-rich N-terminal metal-binding domain. *J Biol Chem* 278:40534–40541.
30. Eren E, González-Guerrero M, Kaufman BM, Argüello JM (2007) Novel Zn^{2+} coordination by the regulatory N-terminus metal binding domain of *Arabidopsis thaliana* Zn^{2+}-ATPase HMA2. *Biochemistry* 46:7754–7764.
31. Mitra B, Sharma R (2001) The cysteine-rich amino-terminal domain of ZntA, a Pb(II)/Zn(II)/Cd(II)-translocating ATPase from *Escherichia coli*, is not essential for its function. *Biochemistry* 40:7694–7699.
32. Sazinsky MH, *et al.* (2007) Characterization and structure of a Zn^{2+} and [2Fe–2S]-containing copper chaperone from *Archaeoglobus fulgidus*. *J Biol Chem* 282:25950–25959.
33. Achila D, *et al.* (2006) Structure of human Wilson protein domains 5 and 6 and their interplay with domain 4 and the copper chaperone HAH1 in copper uptake. *Proc Natl Acad Sci USA* 103:5729–5734.
34. Forbes JR, Hsi G, Cox DW (1999) Role of the copper-binding domain in the copper transport function of ATP7B, the P-type ATPase defective in Wilson disease. *J Biol Chem* 274:12408–12413.
35. Palumaa P, Kangur L, Voronova A, Sillard R (2004) Metal-binding mechanism of Cox17, a copper chaperone for cytochrome c oxidase. *Biochem J* 382:307–314.
36. Wernimont AK, Yatsunyk LA, Rosenzweig AC (2004) Binding of copper(I) by the Wilson disease protein and its copper chaperone. *J Biol Chem* 279:12269–12276.
37. Yang Y, Mandal AK, Bredestón LM, González-Flecha FL, Argüello JM (2007) Activation of *Archaeoglobus fulgidus* Cu(+)-ATPase CopA by cysteine. *Biochim Biophys Acta* 1768:495–501.
38. Toyoshima C, Nomura H (2002) Structural changes in the calcium pump accompanying the dissociation of calcium. *Nature* 418:605–611.
39. Bradford MM (1976) A rapid and sensitive method for the quantification of microgram quantities of protein utilizing the principle of protein-dye binding. *Anal Biochem* 72:248–254.
40. Brenner AJ, Harris ED (1995) A quantitative test for copper using bicinchoninic acid. *Anal Biochem* 226:80–84.
41. Lanzetta PA, Alvarez LJ, Reinach PS, Candia OA (1979) An improved assay for nanomole amounts of inorganic phosphate. *Anal Biochem* 100:95–97.